UNCORRECTED PROOF

Fabrication of CNTs/TiO$_2$ photoanodes for sensitive determination of organic compounds

Q.1 **Lihong Li, Min Yang, Shanqing Zhang**[1]**, Guiying Li, William Wen, Haimin Zhang and Huijun Zhao**

Environmental Futures Centre and Griffith School of Environment Gold Coast Campus, Griffith University, QLD 4222, Australia

E-mail: s.zhang@griffith.edu.au

Abstract

Titanium dioxide (TiO$_2$) and carbon nanotubes (CNTs) are the two most popular functional materials in recent years. In this study, CNTs/TiO$_2$ composite and TiO$_2$ photoanodes were fabricated by a dip-coating technique, followed by subsequent calcination. The resultant photoanodes were characterized by scanning electron microscopy (SEM), x-ray diffraction (XRD), and UV–visible spectroscopy (UV–vis). The results suggest that the carbon nanotubes were successfully incorporated with the TiO$_2$ nanoparticulates without damage and that the resultant TiO$_2$ nanoparticles consisted of anatase and rutile. The CNTs/TiO$_2$ photoanodes were capable of oxidizing various types of organic compounds (e.g. glucose, potassium hydrogen phthalate, and phenol) in aqueous solutions in a photoelectrochemical bulk cell. In comparison with the pure TiO$_2$ photoanode, the sensitivity of the photoanode for the detection of organic compounds has been improved by 64%, while the background current was reduced by 80% due
Q.2 to the introduction of the CNTs. These advantages can be ascribed to the improved adsorptivity to organic compounds, increased absorption of UV light and enhanced electron transport at the CNTs/TiO$_2$ photoanode due to the introduction of the CNTs.

S Online supplementary data available from stacks.iop.org/Nano/21/000000/mmedia

Q.3 (Some figures in this article are in colour only in the electronic version)

1. Introduction

Up to now, titanium dioxide (TiO$_2$) has been a dominant photocatalyst owing to its non-toxic nature, superior photo-corrosion resistance and excellent photocatalytic activity [1]. Various applications of nanostructured photocatalysts have been investigated, and the solar energy conversion and photocatalytic degradation of organic contaminants have been the main focuses [2–4]. Recently, the analytical applications of nanostructured TiO$_2$ have been reported for environmental monitoring in the form of sensor arrays [5, 6]. Nanostructured TiO$_2$ films have been widely used as sensors for various gases, such as H$_2$ [7], O$_2$ [8], CO [9], methanol [10], alcohol vapor [11], humidity measurement [12] and also environmental

pollutants in wastewater [13]. Despite the great potential of these sensors, in order to expand the scope of the sensors toward a wide range of organic and inorganic contaminants, more advances in TiO$_2$ nanostructured materials serving as sensors are much needed [5].

Carbon nanotubes (CNTs)/TiO$_2$ composite systems have attracted much attention in recent years due to the unique properties of CNTs. Taking advantage of the large surface area, extraordinary electrical conductivity, robust mechanical strength and thermal stability of CNTs, the CNTs/TiO$_2$ composite materials have been employed for a wide range of applications concerning energy and the environment [14], such as batteries [15], supercapacitors [16, 17], optoelectronics [18], electrocatalysis [19, 20], photocatalysis [21, 22] and sensing devices [23–27]. In the sensing applications, Llobet *et al* reported that the CNTs/TiO$_2$ hybrid film sensor was

---

[1] Author to whom any correspondence should be addressed.

significantly more sensitive to oxygen than the pure TiO_2 one. Moreover, the hybrid sensors could also be operated at a lower operating temperature (350 °C) than the pure TiO_2 sensors (500 °C) [24]. Ueda *et al* developed the CNTs/TiO_2 hybrid gas sensor towards NO gas, which could be operated at room temperature and showed a good sensitivity [27]. The CNTs/TiO_2 composite materials have also been used in NH_3 sensing [25], H_2O_2 sensing [23], and even biosensing for cancer cells [26].

In these applications, particularly in the sensing system and the photocatalytic degradation of pollutant in water treatment, the enhancements observed in the CNTs composite systems in comparison with the non-hybrid ones can be attributed to several possible merits contributed from CNTs: (i) higher adsorption capacity to reactant species due to the high surface area nature of the CNTs [28, 29]; (ii) photo-excitation under longer wavelength light [28, 29]; (iii) the relatively low recombination of photogenerated electron–hole pairs facilitated by the extraordinary electrical conductivity of the CNTs [30].

In this work, we attempt to incorporate CNTs with TiO_2 photoanodes in order to achieve a more sensitive determination of organic compounds in comparison with the corresponding pure TiO_2 photoanodes. Both the CNTs/TiO_2 and the pure TiO_2 thin film photoanodes were constructed using a dip-coating technique. After a series of calcination processes, the resultant thin film photoanodes were characterized using a scanning electron microscope (SEM), x-ray diffraction (XRD) and a UV–visible spectrophotometer (UV–vis). The hydrophilicity property was appraised by measuring their contact angles. In a photoelectrochemical bulk cell, the resultant CNTs/TiO_2 photoanodes and the pure TiO_2 photoanodes were used to detect low adsorptive compounds with hydroxylic functional group [31, 32], i.e. glucose and phenol, and highly adsorptive compounds with carboxylic functional groups [33], i.e. potassium hydrogen phthalate (KHP). The sensing performances of the CNTs/TiO_2 photoanodes and the pure TiO_2 photoanodes were evaluated and compared.

2. Experimental details

2.1. Chemicals and materials

Indium tin oxide (ITO) conductive glass slides (8 Ω/square) were commercially supplied by Delta Technologies Limited. Titanium butoxide (97%), potassium hydrogen phthalate, D-glucose, phenol, sodium nitrate, isopropyl alcohol, concentrated nitric acid and carbowax 20M (Supelco) were of analytical grade and used as supplied without purification. All the chemicals were purchased from Sigma-Aldrich unless otherwise stated. All the solutions were prepared using high purity deionized water (Millipore Corp., 18 MΩ cm). Multi-walled CNTs were purchased from Shenzhen Nano-Technologies Port Co. Ltd.

2.2. Pre-treatment of CNTs

The CNTs need to be treated with strong acid to avoid agglomeration. Typically, 0.6 g of CNTs was added into 80 ml concentrated HNO_3–H_2SO_4 (1:3, v/v) under constant stirring at 60 °C for 10 h. The mixture was filtered and washed with Milli-Q water until the pH of the filtrate reached 6.0. The pre-treated CNTs were dried at 65 °C in an oven.

2.3. Fabrication and characterization of the pure TiO_2 and CNTs/TiO_2 photoanodes

The TiO_2 colloid was synthesized by the hydrolysis of titanium butoxide [34]. Briefly, 25 ml titanium butoxide with 8 ml isopropanol was added dropwise into 0.1 M nitric acid solution under vigorous stirring at room temperature (23 °C). The slurry was kept in a water bath at 80 °C, stirred and peptized for 10 h. The resultant colloid was hydrothermally treated at 200 °C for 12 h. The solid concentration of TiO_2 was adjusted to 6% (w/w) with water. Carbowax (1.8%, w/w) was added as a binder into the resultant colloid. It is well recognized that the carbowax (polyethylene glycol) is able to improve the mechanical strength and increase the porosity and surface area, from our works and other main stream researches in these fields [35–37]. The pre-treated CNTs (5 wt% with respect to the mass of TiO_2) were subsequently added into this colloid, and sonicated (Digital Sonifer, Branson) for 40 min to improve the interaction between the TiO_2 colloid and CNTs. The ITO glass slides were washed with acetone and then Milli-Q water to assure the cleanliness. The CNTs/TiO_2 colloid was dip-coated onto the ITO substrates, dried in ambient environment and annealed at 450 °C for 0.5 h in air. After cooling, the substrates were dip-coated again and annealed at 700 °C for 2 h in N_2 atmosphere. The pure TiO_2 photoanodes (i.e., the control sample) were also prepared with CNTs-free TiO_2 colloid using the same procedure. The variations of the film thicknesses of the nanomaterials of the TiO_2 photoanode and CNTs/TiO_2 photoanode were 600 nm ± 3% and 600 nm ± 3.5%, respectively. The difference of thickness is therefore negligible.

The surface morphology of the CNTs/TiO_2 photoanode was characterized by scanning electron microscopy (SEM, JSM 890). The crystalline phase of the thin film was determined by an x-ray diffractometer (Bruker) with Cu–Kα radiation. Transmittance spectra were obtained using a UV-1601 spectrophotometer (Shimazu, Japan). The hydrophilic property of the CNTs/TiO_2 thin film was evaluated by means of a commercial contact angle meter (FTA200 Dynamic Contact Angle Analyzer).

2.4. Photoelectrocatalytic degradation of organic compounds

A three-electrode photoelectrochemical system was used to investigate the photoelectrocatalytic oxidation of organic compounds at the TiO_2 and CNTs/TiO_2 photoanodes [34]. The experiments were performed at room temperature (23 °C). A TiO_2 or CNTs/TiO_2 thin film photoanode was used as the working electrode. The working electrode was fitted into an electrode holder with ca. 0.78 cm^2 left unsealed to be exposed to the solution and for UV illumination. A saturated Ag/AgCl electrode and a platinum mesh were used as the reference and auxiliary electrodes respectively. The supporting electrolyte was 0.1 M $NaNO_3$. A voltammograph (CV-27, BAS) was

used to measure the photocurrent under controlled potential and linear sweep voltammetry (LSV) experiments. Potential and current signals were recorded by a PC coupled with a Maclab 400 interface (AD Instruments). A 150 W xenon (HFC-150, TrustTech, Beijing, China) with regulated optical output and a UV-band-pass filter (UG-5, Schott) were placed in front of the quartz window to prevent the testing solution from being heated up. The light intensity at the working electrode surface was controlled at 6.6 mW cm^{-2} in this work, measured at 365 nm wavelength using a UV irradiance meter (UV-A Instruments of Beijing Normal University).

3. Results and discussion

### 3.1. Preparation and materials characterization of the CNTs/TiO$_2$ photoanode

It is well established that the crystallinity of TiO$_2$ plays an essential role in the photocatalytic activity. TiO$_2$ with poor crystallinity, such as amorphous TiO$_2$, normally has low photocatalytic activity due to the severe structural defects that often act as the recombination centers of photogenerated electrons and holes [38]. A simple calcination process at a high temperature (e.g., 450 °C) is an effective way to improve the crystallinity of the TiO$_2$ semiconductor [38]. In our previous study, we synthesized TiO$_2$ colloid via a sol–gel process and fabricated TiO$_2$ thin film using a dip-coating process. It was found that the TiO$_2$ thin film consists of almost 100% anatase TiO$_2$ after a calcination process at 450 °C, while the thin film consists of mixed phases (i.e., anatase and rutile) when it is further treated at a temperature above 700 °C in air [34]. Moreover, the mixed-phase TiO$_2$ shows better photocatalytic degradation ability than pure phase TiO$_2$ thin film [34].

In order to obtain the mixed-phase TiO$_2$ compositions, the dip-coated CNTs/TiO$_2$ composite photoanodes were subjected to a calcination process at 700 °C. The thermal stability of CNTs in air was first investigated. After the thermal treatment at 450 °C in air for 2 h, it was observed that the overall tubular structure of the CNTs still remained intact (see figures 1(a) and (b)). A further thermal treatment at 700 °C in air resulted in a complete decomposition of the CNTs into CO$_2$. This problem was overcome by protecting the photoanodes with high purity N$_2$ in the calcination process. It was found that the appearance of the typical CNTs after being treated at 700 °C in N$_2$ (see figure 1(c)) was identical to that of the untreated CNTs. According to these findings, the as-coated CNTs/TiO$_2$ photoanodes in this work were first calcined at 450 °C in air for 0.5 h in order to remove the carbowax (the binder), achieve strong bindings among the anatase TiO$_2$ particles, CNTs and substrates without damage of CNTs, and improve the crystallinity. The photoanodes were then sintered at 700 °C for 2 h in the N$_2$ atmosphere in an attempt to achieve the partial phase transition from anatase to rutile. The physical properties of TiO$_2$ nanomaterials are influenced by the thermal treatment with different surrounding atmospheres [39]. The crystalline phases of the resultant photoanode from this calcination process (in the N$_2$ atmosphere) which were not investigated previously [34] have been analyzed in this work.

(a)

(b)

(c)
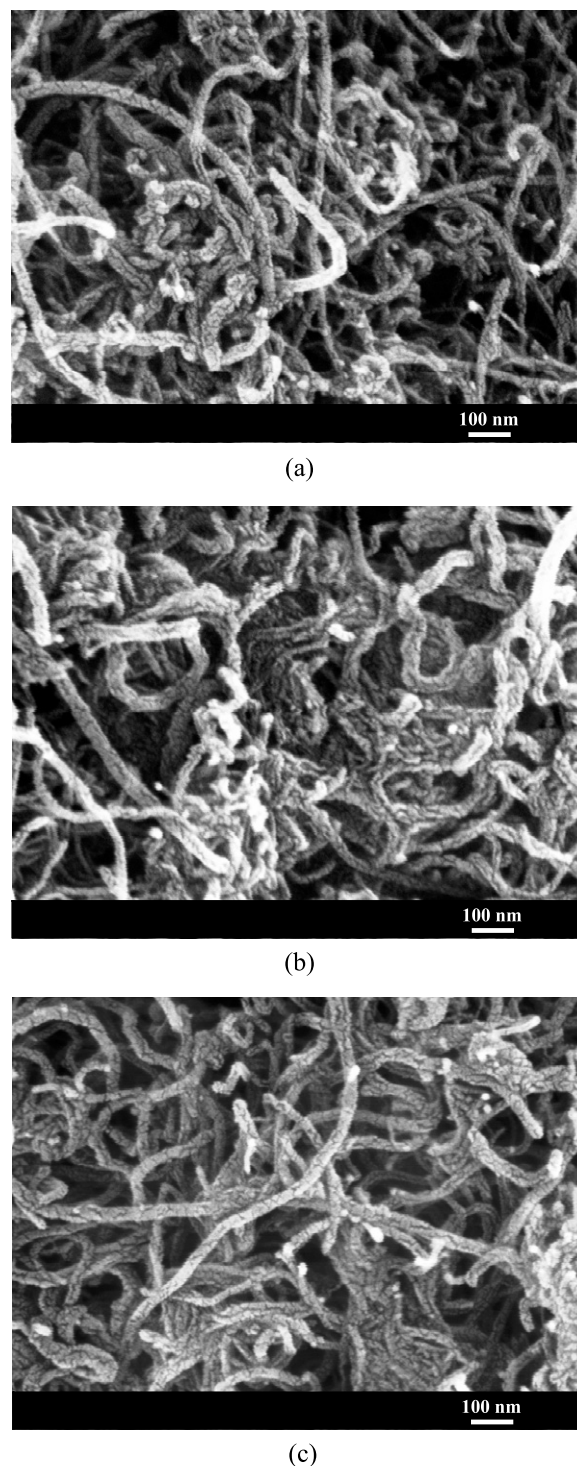
Figure 1. SEM images of CNTs under different thermal treatment conditions: (a) the original CNTs without thermal treatment; (b) the CNTs calcined at 450 °C for 2 h in air; (c) the CNTs calcined at 700 °C for 2 h in N$_2$.

Figure 2 shows the XRD patterns of the pure TiO$_2$ photoanode (curve (a)) and the CNTs/TiO$_2$ photoanode (curve (b)) after 700 °C calcination. It suggests that the introduction of CNTs had no significant effect on the crystallinity of TiO$_2$. Both of the films consist of anatase and rutile, confirmed by characteristic diffraction peaks of anatase
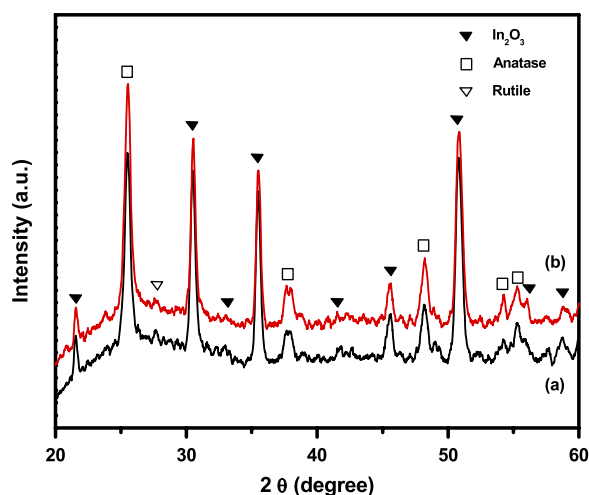
Figure 2. XRD patterns of the pure TiO_2 (a) and CNTs/TiO_2 photoanodes (b), both of them were calcined at 450 °C in air and 700 °C in N_2 protection atmosphere.

at 2θ degrees of 25.50 and rutile at 2θ degrees of 27.68. The CNTs/TiO_2 film contained 93% of anatase and 7% of rutile, while the pure TiO_2 film had a similar ratio (92% of anatase and 8% of rutile). The characteristic peak for CNTs at the position of 26.0 [40] was insignificant, which was consistent with the results in other literatures [28, 30]. This may be attributed to the overlap of the intense peaks of the CNTs (0 0 2) at 2θ degrees of 26.0 and strong anatase (0 0 1) peak at 2θ degrees of 25.5, as the mass of the CNT is only 5% of the mass of the TiO_2 in the CNTs/TiO_2 film.

The surface morphology of the CNTs/TiO_2 film was examined by the SEM, which is shown in figure 3(a). The morphology of the CNTs/TiO_2 film and the within structure of the CNTs/TiO_2 are significantly different from results from Eder and Windle's group [41]. The difference is possibly due to dramatically different experimental conditions. In our work, we used hydrothermal processed highly crystalline TiO_2 nanoparticles with various shape and sizes, different CNTs, different concentrations of CNTs, different CNT treatment methods, carbowax as a binder, and different calcination procedures. In our work, the average TiO_2 particle size of the CNTs/TiO_2 sample is ca. 25–50 nm, which is roughly the same as that of the pure TiO_2 photoanode [34]. This suggests that the addition of the CNTs did not change the particle size and its distribution. It is generally difficult to observe the CNTs from the CNTs/TiO_2 photoanode surface possibly due to the facts that only a relatively small amount of CNTs (e.g., 5% of the TiO_2 nanoparticles) are used, and the CNTs can be strongly incorporated with TiO_2 due to the CNT surfaces being activated by the acid treatment. To observe the distribution of the CNTs, a cross-section sample was therefore prepared and observed under the SEM (see figure 3(b)). It reveals that the CNTs were evenly distributed and well cemented into the TiO_2 film. This observation suggests that the physical structure of the CNTs was well maintained through this 700 °C calcination process and the protection by the N_2 atmosphere was effective. This was consistent with the observation from figure 1. From the above analyses, we can safely conclude that
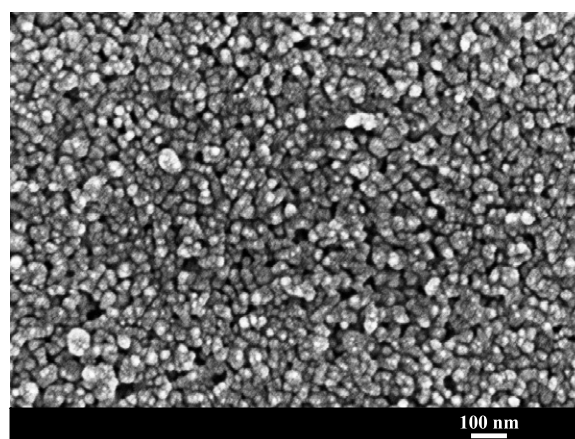

(a)
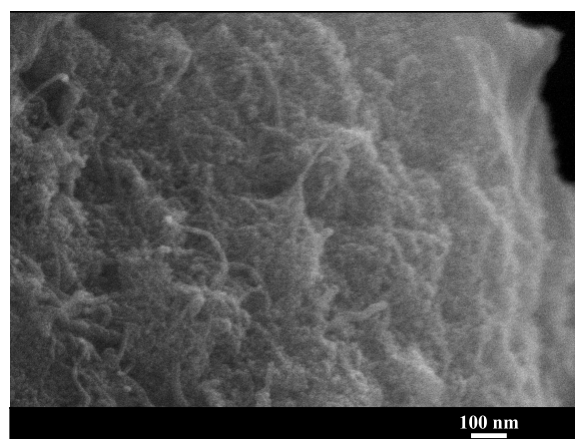
(b)

Figure 3. Top-viewed (a) and cross-sectional (b) SEM images of the CNTs/TiO_2 photoanode after the calcination processes at 450 °C in air and 700 °C in N_2 protection atmosphere.

the CNTs/TiO_2 mixed-phase photoanode and the pure TiO_2 mixed-phase photoanode can be obtained via the calcination process at 700 °C in N_2 protection atmosphere.

The UV–vis transmittance spectra of the ITO glass (curve (a)), the pure TiO_2 (curve (b)) and CNTs/TiO_2 photoanodes (curve (c)) are presented in figure 4. Curve (a) indicates that the aluminosilicate ITO glass has no absorption in the visible light and near UV region. Curve (b) shows that the band edge absorption of the TiO_2 was at ca. 390 nm, typical for anatase. Compared with curve (b), the absorption edge of curve (c) was shifted into the visible light region significantly due to the introduction of CNTs. Because pure CNTs have significant absorbance over the entire visible light region [42], wide optical absorptions in the visible light region are also observed for the CNTs/TiO_2 photoanode.

Besides the absorption, the surface properties such as hydrophilicity of the TiO_2 surface could be affected by the introduction of the CNTs as well. The change of the hydrophilicity can be reflected by the variation of the contact angle with pure water. The measured contact angles were 60.2° and 36.3° on the pure TiO_2 film and the CNTs/TiO_2 film respectively, indicating a significant increase in hydrophilicity
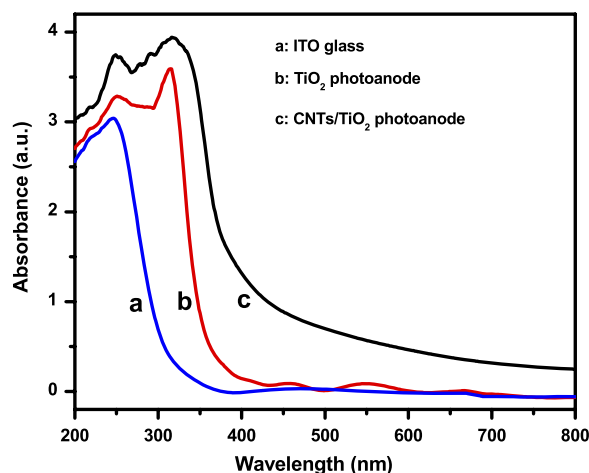
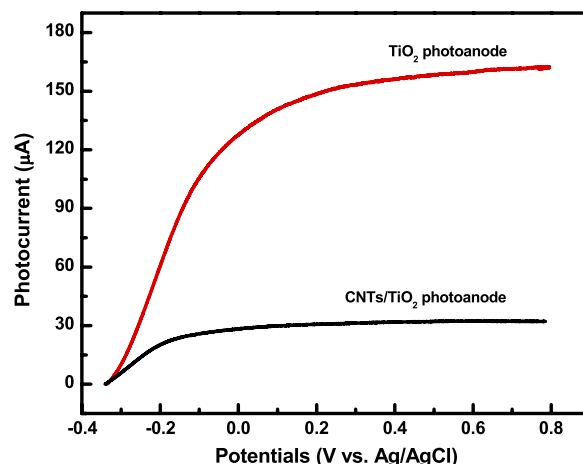**Figure 4.** UV–vis absorption spectra of ITO glass substrate (a), pure TiO$_2$ photoanode (b) and CNTs/TiO$_2$ photoanode (c).

Figure 5. Voltammograms of the pure TiO$_2$ photoanode and CNTs/TiO$_2$ photoanode in 0.1 M NaNO$_3$ electrolyte under UV illumination.

by the introduction of the CNTs. This is probably due to several reasons. Firstly, the acid pre-treatment which involves the oxidation of the CNTs and formation of hydrophilic functional groups (e.g. hydroxyl, carboxyl, and carbonyl) on the CNTs' surface [43]. Secondly, the TiO$_2$ film is porous due to the use of carbowax. Thirdly, the TiO$_2$ and CNTs/TiO$_2$ film are very thin (i.e., only 600 nm). When the water solution is applied on the surface of the photoanodes, water molecules are able to reach the internal structure, i.e., the hydrophilic CNTs' surface, leading to the increase of the surface hydrophilicity. The hydrophilic surface favors the adsorption of hydrophilic organic compounds, which may benefit the adsorption process of the organic compounds during the photocatalytic oxidation at the CNTs/TiO$_2$ photoanode.

3.2. Photoelectrochemical oxidation of water

The photoelectrocatalytic oxidation of water was first investigated since the response of the photocurrent resulting from the oxidation or reduction of water may influence the electrochemical measurements in aqueous solutions. Figure 5 shows the voltammograms recorded at the pure TiO$_2$ and CNTs/TiO$_2$ photoanodes in 0.1 M NaNO$_3$ (as electrolyte) under the same UV illumination intensity. It can be seen that for both photoanodes, the photocurrent increased with the applied potential bias at low potential range (-0.4 to $+0.2$ V) then leveled off at more positive potentials (greater than $+0.2$ V). The initial increase in the photocurrents was because the overall reactions at both photoanodes were under the control of the electron transfer process. The increased potential will produce increased electric field to draw electrons from the photoanode surface to the conductive back contact. The photocurrent leveling off at higher potentials (greater than $+0.2$ V) was due to the transportation of electroactive substance (i.e., H$_2$O) from the bulk to the photoanode surface becoming the limiting step. It was found that the potential $+0.3$ V was able to provide sufficient electric field to collect electrons generated from the catalytic reactions at the surface. Therefore, the collection of the electrons will no longer be the
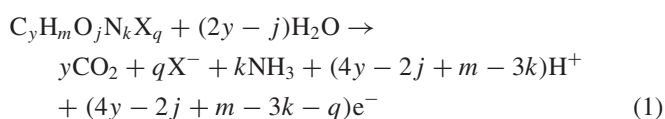
limiting step and the further increase of potential will not lead to significant increase of the photocurrent. In this scenario, the magnitude of the photocurrent can be used to represent the photocatalytic activity of the photoanode. As shown in figure 5 under the same potential bias and experimental conditions, the photocurrent of the CNTs/TiO$_2$ photoanode was about 20% of the photocurrent of the pure TiO$_2$ photoanode, suggesting that the photocatalytic oxidation of water at the photoanode had been reduced by 80% due to the introduction of the CNTs compared with the pure TiO$_2$ photoanode. From the viewpoint of analytical chemistry, the water oxidation current is commonly considered as the background current. Therefore, the characteristic of low background current will be an advantage of the CNTs/TiO$_2$ photoanode over the pure TiO$_2$ current.

3.3. Photoelectrocatalytic oxidation of organic compounds

The general electrochemical equation for complete mineralization of an organic compound, C$_y$H$_m$O$_j$N$_k$X$_q$, on a TiO$_2$ electrode can be represented as in equation (1) [44]:

$$C_yH_mO_jN_kX_q + (2y - j)H_2O \rightarrow$$
$$yCO_2 + qX^- + kNH_3 + (4y - 2j + m - 3k)H^+$$
$$+ (4y - 2j + m - 3k - q)e^- \qquad (1)$$

where X represents a halogen atom. The electron transfer number (n) in the complete mineralization of the organic compound is equal to $4y - 2j + m - 3k - q$.

Glucose, phenol and KHP were selected to study the photoelectrochemical performance of the CNTs/TiO$_2$ and TiO$_2$ photoanodes. Because it can be seen from section 3.2 that the mass transport of electroactive substance (i.e. H$_2$O) from the bulk to the photoanode surface became the limiting step when the potential bias was higher than $+0.2$ V (see figure 5), a potential bias of $+0.3$ V was chosen for subsequent photoelectrocatalytic experiments to obtain a steady state current. At this potential, the recombination of photoinduced electron–hole pairs was sufficiently suppressed. Two sets
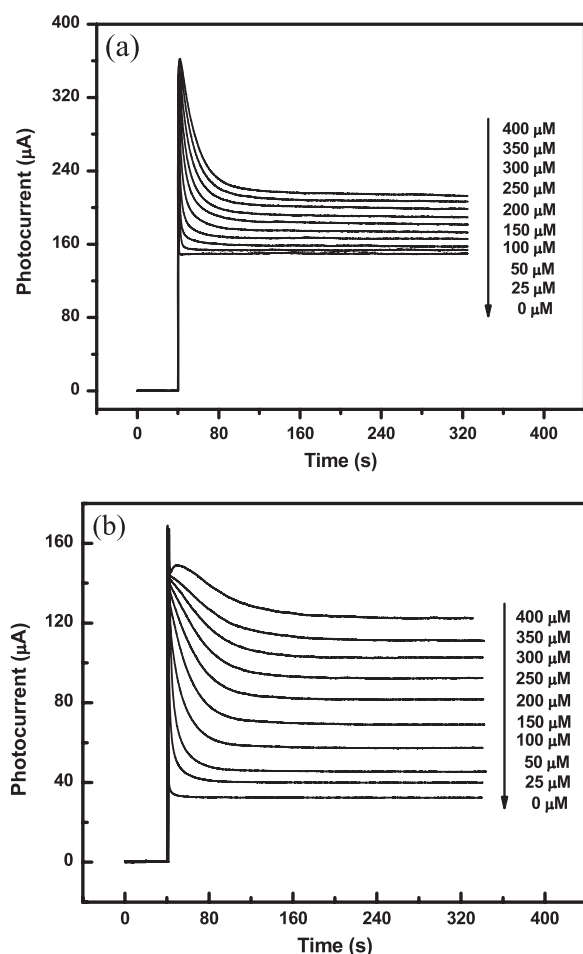
Figure 6. Typical photocurrent responses of the pure TiO$_2$ photoanode (a) and the CNTs/TiO$_2$ photoanode (b) to different concentrations of glucose.

of photocurrent–time profiles of the pure TiO$_2$ photoanode (see figure 6(a)) and CNTs/TiO$_2$ photoanode (see figure 6(b)) were obtained from solutions containing 0.1 M NaNO$_3$ and different concentrations of glucose under the UV illumination, respectively. For the blank solution (0.1 M NaNO$_3$), where the glucose concentration was zero, the photocurrent went up quickly and then leveled off and eventually a steady state current was obtained, named as i_{blank}. For all glucose concentrations in figures 6(a) and (b), the photocurrents increased rapidly to a peak value and decayed to the steady state, which was nominated as i_{total}. Moreover, an abrupt spike in the photocurrent (in a time domain of 1 s) was observed for the CNTs/TiO$_2$ photoanode but not for the pure TiO$_2$ one. This spike may result from the pre-adsorbed water and glucose at the CNTs/TiO$_2$ photoanode. This pre-adsorption phenomenon was much less significant at the pure TiO$_2$ photoanode. This difference implies that the adsorptive property of the CNTs/TiO$_2$ photoanode to water and glucose is stronger than that of the pure TiO$_2$ photoanode. This might be related to the aforementioned difference of the surface hydrophilicity.

It is well established that the steady state photocurrent for the blank solution (i_{blank}) originated from the photo-

electrocatalytic oxidation of water, while the steady state photocurrent for the glucose solutions (i_{total}) was generated from the oxidation of water and glucose [44]. A net steady state photocurrent (i_{net}), originated from the oxidation of glucose, can be obtained by subtracting i_{blank} from i_{total} as in equation (2). i_{net} can be used to represent the oxidation rate of the corresponding organic compound and also quantify the concentration of organic compounds in aqueous samples [44]. Therefore, higher net current when oxidizing organic compounds suggests a faster oxidation rate of the organic compounds in terms of oxidation kinetics and higher sensitivity in terms of analytical performance:

$$i_{net} = i_{total} - i_{blank}. \qquad (2)$$

Using equation (2), the i_{net} values of different photoanodes can be obtained from figures 6(a) and (b) and plotted against the glucose concentration as shown in figure 7(a). Good linear relationships between the glucose concentration and i_{net} were obtained from both photoanodes, indicating the both photoanodes are promising in the sensing application. The slope of the i_{net}–[glucose] calibration curve indicates the photoelectrocatalytic activity towards glucose oxidation. It is notable that the obtained slope value of the CNTs/TiO$_2$ photoanode is larger than that of the pure TiO$_2$ photoanode, demonstrating that the photoelectrocatalytic activity of the CNTs/TiO$_2$ photoanode towards glucose oxidation was better than that of the pure TiO$_2$ photoanode.

Similarly, the CNTs/TiO$_2$ photoanode and the pure TiO$_2$ photoanode were used to detect phenol and KHP in 0.1 M NaNO$_3$ aqueous solution. The obtained i_{net} values were plotted against [phenol] and [KHP] as shown in figures 7(b) and (c), respectively. At both the CNTs/TiO$_2$ and pure TiO$_2$ photoanodes, good linear relationships were also observed for both phenol and KHP. More importantly, the slope values obtained from the CNTs/TiO$_2$ photoanode were larger than those from the pure TiO$_2$ photoanode. This suggests that the CNTs/TiO$_2$ photoanode possesses better photocatalytic activity towards phenol and KHP oxidation than the pure TiO$_2$ photoanode.
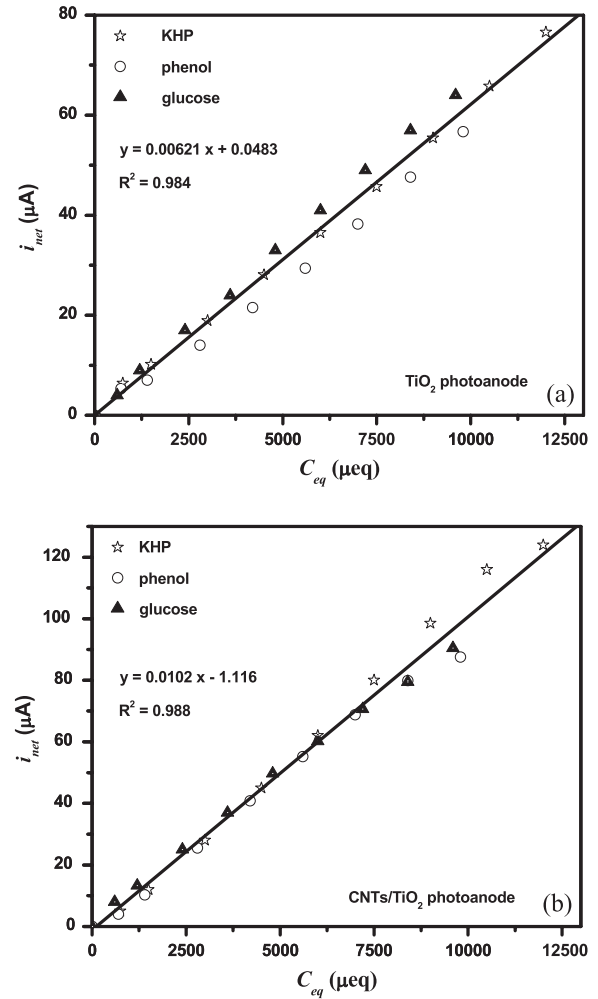
Interesting results were obtained when the i_{net} in figure 7 were plotted against the equivalent concentrations (C_{eq}) of all the organic compounds investigated. The equivalent concentration can be obtained by multiplying the electron transfer number (n) with the corresponding molar concentration (C_M), $C_{eq} = nC_M$ [34]. According to equation (1), the n values of phthalic acid (i.e. KHP), phenol and glucose are 30, 28 and 24, respectively. Excellent linear relationships between i_{net} and C_{eq} were obtained at both the pure TiO$_2$ and CNTs/TiO$_2$ photoanodes (see figures 8(a) and (b)). This is because the photocurrents were under the diffusion control of the organic compounds from the bulk solution to the photoanode surface. It is also remarkable that the slope of the CNTs/TiO$_2$ photoanode (i.e., 0.0102) was much larger than that of the pure TiO$_2$ photoanode (0.006 21). In order words, the sensitivity of the CNTs/TiO$_2$ photoanode for the detection of the organic compounds has been improved by 64% in comparison with the pure TiO$_2$ photoanode. This is
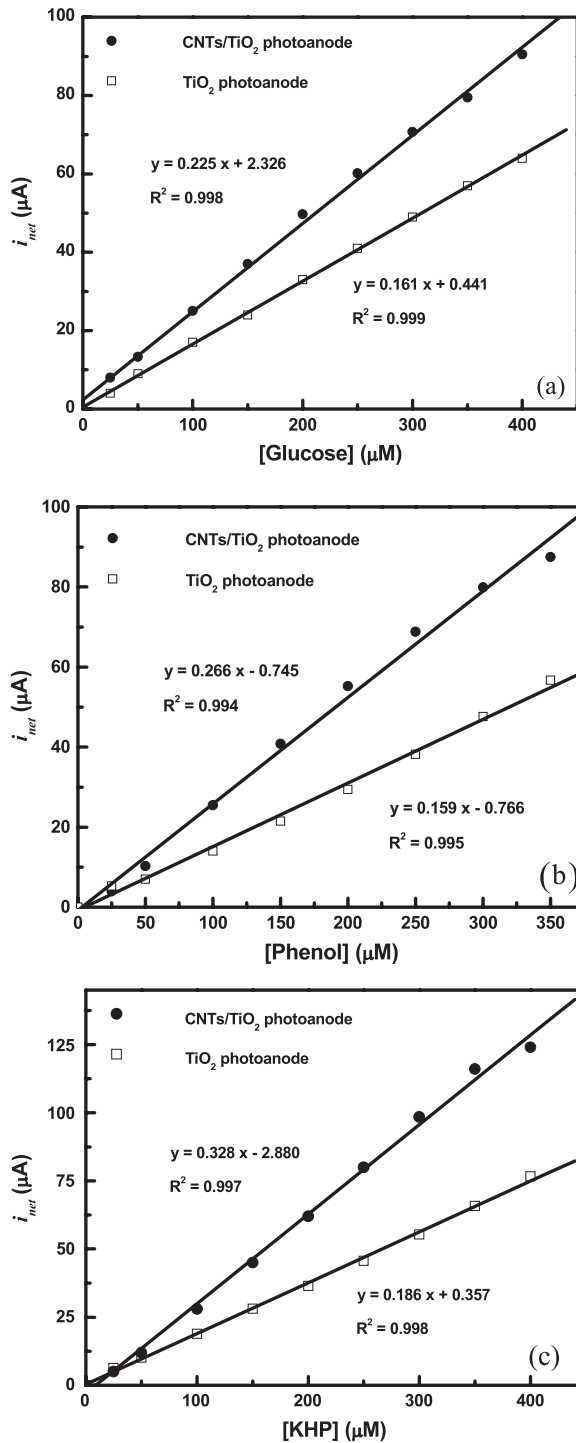
Figure 7. Plots of net photocurrent i_{net} against glucose (a), phenol (b) and KHP (c) for the pure TiO$_2$ and CNTs/TiO$_2$ photoanodes, respectively.

Figure 8. Relationship between i_{net} and C_{eq} at the pure TiO$_2$ (a) and CNTs/TiO$_2$ (b) photoanodes, where $C_{eq}(\mu eq) = nC_M(\mu M)$.

due to the 700 °C thermal treatment process in N$_2$ atmosphere and/or the introduction of CNTs.

According to the XRD spectra we obtained, the crystalline compositions (i.e., anatase and rutile ratio) of the TiO$_2$ photoanode and CNTs/TiO$_2$ photoanode are very similar. In other words, the presence of the CNTs did not affect the rutile formation process in our work, which differs from

a report in the literature [45]. This is probably due to numerous reasons: the use of carbowax binder, different CNTs, different shape (particles versus TiO$_2$ nanotubes in the literature) and different CNT treatment method, and relatively shorter treatment time in our application (2 h compared with 4 h in the literature). Also the doped nitrogen in the TiO$_2$ was not observed for both the TiO$_2$ and CNTs/TiO$_2$ photoanodes according to their x-ray photoelectron spectroscopy (XPS) spectra (see figure S2 available at stacks.iop.org/Nano/21/000000/mmedia). Furthermore, the photocurrent was not obtained for both the TiO$_2$ and CNTs/TiO$_2$ photoanodes under visible light. All of these eliminate the doping of nitrogen into the TiO$_2$ lattice in our case. It can be concluded that the doping of N in the presence of the CNTs should not be responsible for the significant increase of the sensitivity of the CNTs/TiO$_2$ photoanode in this work.

The increase of sensitivity of the CNTs/TiO2 photoanode, therefore, should result from the improved conductivity for electrons, i.e., enhanced electron transport or electron collection efficiency due to the extraordinary conductivity of the CNTs [46]. The CNTs interlinked with the TiO$_2$ nanoparticles can act as 'electron transport superhighways';

therefore, the CNTs are able to facilitate the transport of the photogenerated electrons to the conducting substrate, and subsequently improve the electron collection efficiency and electron–hole separation percentage. This argument can be supported by the results from electrochemical impedance spectroscopy (EIS) measurement under UV illumination (see figure S1 available at stacks.iop.org/Nano/21/000000/mmedia). It is well established that EIS is very effective for investigation of the properties of the electron transfer process across the TiO_2–electrolyte interfaces under light [47]. The smaller impedance arc radius in Nyquist plots indicates faster electron transfer. As shown in figure S1 (available at stacks.iop.org/Nano/21/000000/mmedia), the impedances of the TiO_2 and the CNTs/TiO_2 film are measured as around 1062 Ω and 556 Ω, respectively. In other words, the electron transport ability of the CNTs/TiO_2 photoanode is better than that of the pure TiO_2 photoanode.

Q.6 Thus, it can be concluded that at a given concentration of a given organic compound, more sensitive response in i_{net} can be obtained at the CNTs/TiO_2 photoanode than the pure TiO_2 photoanode. This could be mainly due to the introduction of CNTs, which leads to the improved adsorptivity to organic compounds, increased absorption of UV light and improved electron transport and collection efficiency. For analytical chemistry, the incorporation of the CNTs into the TiO_2 has led to a larger detection current and higher sensitivity.

4. Conclusions

CNTs/TiO_2 photoanodes and pure TiO_2 photoanodes (as the control) were prepared, characterized and used for the detection of organic compounds. The CNTs have been successfully incorporated into the TiO_2 nanostructure in the fabrication process of CNTs/TiO_2 photoanodes. The TiO_2 particles on the resultant photoanodes have anatase and rutile mixed phases. The introduction of the CNTs into the TiO_2 has increased the absorption of UV light, enhanced the hydrophilicity of the TiO_2 surface and improved the electron collection efficiency. When the CNTs/TiO_2 photoanode was used in detecting organic compounds, the net photocurrents were directly proportional to the concentration of organics. In comparison with the pure TiO_2 photoanodes, the CNTs/TiO_2 photoanodes have the advantages of high sensitivity and low background current in the determination of organic compounds in aqueous solutions.

Acknowledgments

Q.7 ## References

[1] Carp O, Huisman C L and Reller A 2004 *Prog. Solid State Chem.* **32** 33–177

[2] Abrams B L and Wilcoxon J P 2005 *Crit. Rev. Solid State Mater. Sci.* **30** 153–82

[3] Fujishima A, Zhang X and Tryk D A 2007 *Int. J. Hydrog. Energy* **32** 2664–72

[4] Hashimoto K, Irie H and Fujishima A 2005 *Japan. J. Appl. Phys.* **44** 8269–85

[5] Chen X and Mao S S 2007 *Chem. Rev.* **107** 2891–959

[6] Hu X, Li G and Yu J C 2009 *Langmuir* **26** 3031–9

[7] Chen Q, Xu D, Wu Z and Liu Z 2008 *Nanotechnology* **19** 365708

[8] Lu H F, Li F, Liu G, Chen Z G, Wang D W, Fang H T, Lu G Q, Jiang Z H and Cheng H M 2008 *Nanotechnology* **19** 405504

[9] Birkefeld L D, Azad A M and Akbar S A 1992 *J. Am. Ceram. Soc.* **75** 2964–8

[10] Sun L, Huo L, Zhao H, Gao S and Zhao J 2006 *Sensors Actuators* B **114** 387–91

[11] Manera M G, Davide Cozzoli P, Leo G, Lucia Curri M, Agostiano A, Vasanelli L and Rella R 2007 *Sensors Actuators* B **126** 562–72

[12] Zhang Y, Fu W, Yang H, Qi Q, Zeng Y, Zhang T, Ge R and Zou G 2008 *Appl. Surf. Sci.* **254** 5545–7

[13] Xu Z and Yu J 2010 *Nanotechnology* **21** 245501

[14] Eder D 2010 *Chem. Rev.* **110** 1348–85

[15] Moriguchi I, Hidaka R, Yamada H, Kudo T, Murakami H and Nakashima N 2006 *Adv. Mater.* **18** 69–73

[16] Frank O, Kalbac M, Kavan L, Zukalova M, Prochazka J, Klementova M and Dunsch L 2007 *Phys. Status Solidi* b **244** 4040–5

[17] Reddy A L M and Ramaprabhu S 2007 *J. Phys. Chem.* C **111** 7727–34

[18] Kongkanand A, Martinez Dominguez R and Kamat P V 2007 *Nano Lett.* **7** 676–80

[19] Song H, Qiu X and Li F 2008 *Electrochim. Acta* **53** 3708–13

[20] Song H, Qiu X, Li F, Zhu W and Chen L 2007 *Electrochem. Commun.* **9** 1416–21

[21] Yao Y, Li G, Ciston S, Lueptow R M and Gray K A 2008 *Environ. Sci. Technol.* **42** 4952–7

[22] Bouazza N, Ouzzine M, Lillo-Ródenas M A, Eder D and Linares-Solano A 2009 *Appl. Catal.* B **92** 377–83

[23] Jiang L-C and Zhang W-D 2009 *Electroanalysis* **21** 988–93

[24] Llobet E *et al* 2008 *Nanotechnology* **19** 375501

[25] Sánchez M and Rincón M E 2009 *Sensors Actuators* B **140** 17–23

[26] Shen Q, You S-K, Park S-G, Jiang H, Guo D, Chen B and Wang X 2008 *Electroanalysis* **20** 2526–30

[27] Ueda T, Takahashi K, Mitsugi F and Ikegami T 2009 *Diamond Relat. Mater.* **18** 493–6

[28] Gao B, Chen G Z and Li Puma G 2009 *Appl. Catal.* B **89** 503–9

[29] Woan K, Pyrgiotakis G and Sigmund W 2009 *Adv. Mater.* **21** 2233–9

[30] Yu Y, Yu J C, Yu J-G, Kwok Y-C, Che Y-K, Zhao J-C, Ding L, Ge W-K and Wong P-K 2005 *Appl. Catal.* A **289** 186–96

[31] Mills G and Hoffman M R 1993 *Environ. Sci. Technol.* **27** 1681–9

[32] Solarska R, Rutkowskal I, Morand R and Augustynski J 2006 *Electrochim. Acta* **51** 2230–6

[33] Chen J, Ollis D F, Rulkens W H and Bruning H 1999 *Water Res.* **33** 669–76

[34] Jiang D L, Zhang S Q and Zhao H J 2007 *Environ. Sci. Technol.* **41** 303–8

[35] Benkstein K D, Kopidakis N, van de Lagemaat J and Frank A J 2003 *J. Phys. Chem.* B **107** 7759–67

[36] Kalyanasundaram K and Grätzel M 1998 *Coord. Chem. Rev.* **177** 347–414

[37] Saito Y, Kambe S, Kitamura T, Wada Y and Yanagida S 2004 *Sol. Energy Mater. Sol. Cells* **83** 1–13

[38] Zhang Q, Gao L and Guo J 2000 *Appl. Catal.* B **26** 207–15

[39] Zhang H, Xie C, Zhang Y, Liu G, Li Z, Liu C, Ma X and Zhang W F 2008 *J. Appl. Phys.* **103** 103107

[40] An G, Ma W, Sun Z, Liu Z, Han B, Miao S, Miao Z and Ding K 2007 *Carbon* **45** 1795–801

[41] Eder D and Windle A H 2008 *J. Mater. Chem.* **18** 2036–43

[42] Xie Y, Heo S, Yoo S, Ali G and Cho S 2010 *Nanoscale Res. Lett.* **5** 603–7

[43] Yan X-b, Tay B K and Yang Y 2006 *J. Phys. Chem.* B **110** 25844–9

[44] Zhang S, Li L and Zhao H 2009 *Environ. Sci. Technol.* **43** 7810–5

[45] Eder D, Kinloch I A and Windle A H 2006 *Chem. Commun.* 1448–50

[46] Raffaelle R P, Landi B J, Harris J D, Bailey S G and Hepp A F 2005 *Mater. Sci. Eng.* B **116** 233–43

[47] Yu H, Quan X, Chen S, Zhao H and Zhang Y 2008 *J. Photochem. Photobiol.* A **200** 301–6

Queries for IOP paper 362824

Journal: **Nano**
Author: **L Li et al**
Short title: **Fabrication of** CNTs/TiO$_2$ **photoanodes for sensitive determination of organic compounds**

Page 1

Query 1:

    Author: Please check the author names and affiliations carefully.

Query 2:

    Author: 'In comparison with the pure TiO$_2$ photoanode' was repeated in this sentence. The apparent duplication has been removed. Please check the edited version, and correct if necessary.

Query 3:

    Author: Please be aware that the colour figures in this article will only appear in colour in the Web version. If you require colour in the printed journal and have not previously arranged it, please contact the Production Editor now.

Page 2

Query 4:

    Author: Please check the edits made in the sentence 'It is well recognized that the carbowax...', and correct if necessary.

Page 4

Query A:

    Author: Do you mean 'protective atmosphere' here and in two other places?

Query 5:

    Author: Please clarify 'within structure'. Do you mean 'internal structure'?

Page 8

Query 6:

    Author: Please check/confirm 'organic compound' here. Please check.

Query 7:-

    Author: Please check the details for any journal references that do not have a blue link as they may contain some incorrect information. Pale purple links are used for references to arXiv e-prints.